

## BRIEF COMMUNICATION

**Antioxidants inhibit neuronal toxicity in Parkinson's disease-linked LRRK2**Dario C. Angeles<sup>1,2</sup>, Patrick Ho<sup>3</sup>, Brian W. Dymock<sup>4</sup>, Kah-Leong Lim<sup>3,5,6</sup>, Zhi-Dong Zhou<sup>1</sup> & Eng-King Tan<sup>1,3,6</sup><sup>1</sup>Department of Neurology, Singapore General Hospital, 20 College Rd, The Academia Discovery Tower, Singapore, 169856<sup>2</sup>Departments of Psychology and Pediatrics, National University of Singapore, Singapore<sup>3</sup>National Neuroscience Institute, 11 Tan Tock Seng, Singapore, 308433<sup>4</sup>Department of Pharmacy, National University of Singapore, 21 Lower Kent Ridge, Singapore, 119077<sup>5</sup>Department of Physiology, National University of Singapore, 21 Lower Kent Ridge, Singapore, 119077<sup>6</sup>Duke-NUS Graduate Medical School, 8 College Rd, Singapore, 169857**Correspondence**

Eng-King Tan, Department of Neurology, Singapore General Hospital, 20 College Rd, The Academia Discovery Tower, Singapore 169856. Tel: +6563265003; Fax: +6562203321; E-mail: gnrtek@sgh.com.sg

**Funding Information**

This work was supported by the National Medical Research Council.

Received: 5 July 2015; Revised: 28 October 2015; Accepted: 24 November 2015

*Annals of Clinical and Translational Neurology* 2016; 3(4): 288–294

doi: 10.1002/acn3.282

**Introduction**

Parkinson's disease (PD) is a common age-related neurodegenerative disease that manifests as motor and non-motor dysfunction.<sup>1</sup> Pathologically, it leads to loss of dopamine (DA) neurons in the substantia nigra and formation of intracytoplasmic inclusions termed Lewy bodies, mainly of misfolded  $\alpha$ -synuclein in the filaments.<sup>2</sup> Medications and surgical therapies relieve symptoms<sup>3</sup>; however, no definitive preventive neuroprotective or disease-modifying cure is available.

Numerous monogenic forms of PD have been identified with mutations in leucine-rich repeat kinase-2 (LRRK2) as the most common cause of sporadic and familial PD.<sup>4</sup> Mutations in several genes cause recessive juvenile parkinsonism, whereas  $\alpha$ -synuclein and LRRK2 are linked with the dominant form of the disease.<sup>3</sup> LRRK2 is a complex protein with the catalytic domain mutations implicated in the

**Abstract**

Mutations in leucine-rich repeat kinase-2 are the most common cause of familial Parkinson's disease. The prevalent G2019S mutation increase oxidative, kinase and toxic activity and inhibit endogenous peroxidases. We initially screened a library of 84 antioxidants and identified seven phenolic compounds that inhibited kinase activity on leucine-rich repeat kinase-2 substrates. The representative antioxidants (piceatannol, thymoquinone, and esculetin) with strong kinase inhibitor activity, reduced loss in dopaminergic neurons, oxidative dysfunction, and locomotor defects in G2019S-expressing neuronal and *Drosophila* models compared to weak inhibitors. We provide proof of principle that natural antioxidants with dual antioxidant and kinase inhibitor properties could be useful for leucine-rich repeat kinase-2-linked Parkinson's disease.

pathogenesis of PD. The common G2019S mutation is associated with increased kinase activity and causes defects in cytoskeletal structure, autophagy, ArfGAP1-mediated GTPase activity, synaptic vesicle transport, and other pathways.<sup>5–9</sup> Such deleterious roles traversing diverse pathways made LRRK2 a compelling target for drug discovery. However, discovery efforts for small molecule inhibitor of LRRK2 face considerable challenges due to issues on drug specificity, off-target effects, toxicity, and bioavailability in the brain.<sup>10</sup>

Recently, we have shown that LRRK2-G2019S induce oxidative stress and injury via phospho-inactivation of an endogenous mitochondrial antioxidant capable of regulating LRRK2 actions.<sup>11</sup> Here, we evaluate antioxidants that are present in plants or food for their effects on LRRK2 activities using in vitro and in vivo models. We hypothesize that natural dietary antioxidants with less toxicity concerns and with potential kinase inhibitor properties may be targets in LRRK2-linked PD.

## Materials and Methods

The study has been approved by the Singhealth/Singapore General Hospital IRB.

### Reagents and cell viability

The Screen-Well Redox Library was purchased from Enzo Life Sciences (Ann Arbor, MI) while LRRK2 variants were from Life Technologies (Carlsbad, CA). Affinity purification of recombinant LRRK2 and transfection protocols were performed as described.<sup>11</sup> SK-N-SH obtained from ATCC and primary cortical neuronal lines from Lonza (Basel, Switzerland) were maintained according to supplier's protocol. Viability was determined based on the conversion of MTT to insoluble formazan by live cells (Life Technologies). Briefly, cells were grown in 96-well plate to  $1 \times 10^5$  cells/mL and then treated with antioxidants at 0.5  $\mu\text{mol/L}$  or in gradient concentration for 24 h in 2% FBS (Fetal Bovine Serum) media without sodium pyruvate. MTT solution was added for 4 h before samples were collected and measured at OD<sub>570 nm</sub>.

### Radiometric kinase assays

The assays were conducted as described.<sup>11,12</sup> Briefly, 40  $\mu\text{L}$  reactions containing 0.8  $\mu\text{g}$  LRRK2 (Life Technologies, Carlsbad, CA), 1  $\mu\text{g}$  myelin basic protein (MBP) or 5  $\mu\text{g}$  synthetic peptide (Sabio, Singapore), 10  $\mu\text{Ci}$  [ $\gamma$ -<sup>32</sup>P] ATP, and 1X kinase buffer with or without 2  $\mu\text{mol/L}$  of each antioxidant for the screening, were incubated at 30°C for 20 mins then stopped by the addition of LDS sample buffer at 100°C for 5 mins. Samples were resolved by 4–12% sodium dodecyl sulphate polyacrylamide gel electrophoresis (SDS-PAGE) and autoradiography then analyzed using ImageQuant TL software (GE Healthcare Life Sciences, Pittsburgh, PA). In the filter-binding assay, 10  $\mu\text{L}$  of peptide reaction was applied onto P81 phosphocellulose disks followed by two washes in 75 mmol/L phosphoric acid and immersion in scintillant cocktail. Radioactivity was measured using the MicroBeta liquid scintillation counter (PerkinElmer, Waltham, MA).

### *Drosophila* stocks, manipulation, and assays

Promoter lines containing *elav*-GAL4, *ddc*-GAL4 were obtained from Bloomington Stock Center. The generation of human LRRK2 transgenic lines was described previously.<sup>13</sup> hLRRK2 was amplified from pCDNA3.1 constructs and cloned directionally into XhoI–EcoRI site of pUAST vector. The sequence-verified constructs were microinjected into w118 embryos by BestGene. Transgenic flies of genotypes *ddc-GAL4/+* and *ddc-GAL4-hLRRK2 G2019S*

were routinely raised and maintained at 25°C on staple cornmeal media that were replaced every 2 days. Antioxidant in DMSO (Dimethyl Sulfoxide) was incorporated into staple food at an optimal dosage concentration of 10  $\mu\text{mol/L}$ . The fly head homogenate was prepared in RIPA buffer and precleared by centrifugation for use in assays. Immunostaining was performed on the whole-mount adult fly brains. The dissected brains were probed with rabbit TH- (1:200; Sigma-Aldrich, St. Louis, MO) or rat *elav*- (1:50; Developmental Studies Hybridoma Bank, Iowa City, IA) specific primary antibodies. The number of DA neurons in different clusters was scored under confocal microscopy. Six brain sections from cohorts of five flies per genotype were analyzed using the Nikon NS Element AR 3.2 software (Melville, NY).

For the climbing assay, motor ability was assessed at 15 min intervals using the negative geotaxis assay. Three cohorts of age-matched control flies were anesthetized and placed in a vertical plastic column. After a 1 h recovery period, the percentage of flies that climb to or above the top column line in 1 min was calculated. Triplicate trials were performed in each experiment at 15 min intervals.

### Oxidative state assays

The levels of peroxide and peroxidase activity were measured according to the Amplex Red Kit protocol (Life Technologies). Briefly, reactions containing 50 mmol/L reagent and 1 mg of fly head lysate were incubated for 30 min at room temperature to measure peroxide levels. The peroxidase activity was measured with the addition of 1 mmol/L H<sub>2</sub>O<sub>2</sub>. Fluorescence intensity was measured at Ex/Em 530/590 nm.

### Statistical analysis

Unless specified, data are mean  $\pm$  SEM from three independent triplicate experiments with values between groups compared by Student's *t* test using the GraphPad Prism (La Jolla, CA). Statistical significance was defined at  $P < 0.05$ .

## Results

### Kinase activity of LRRK2

We first assessed the activity of LRRK2 variants using direct kinase assay. The kinase-dead (KD) variant D1994A with mutation in the catalytic pocket had no activity while kinase domain mutants LRRK2-G2019S and -I2020T exhibited a threefold increase in autophosphorylation compared to wild type (Fig. 1A). Incremental amounts of ATP increased the level of phosphorylated

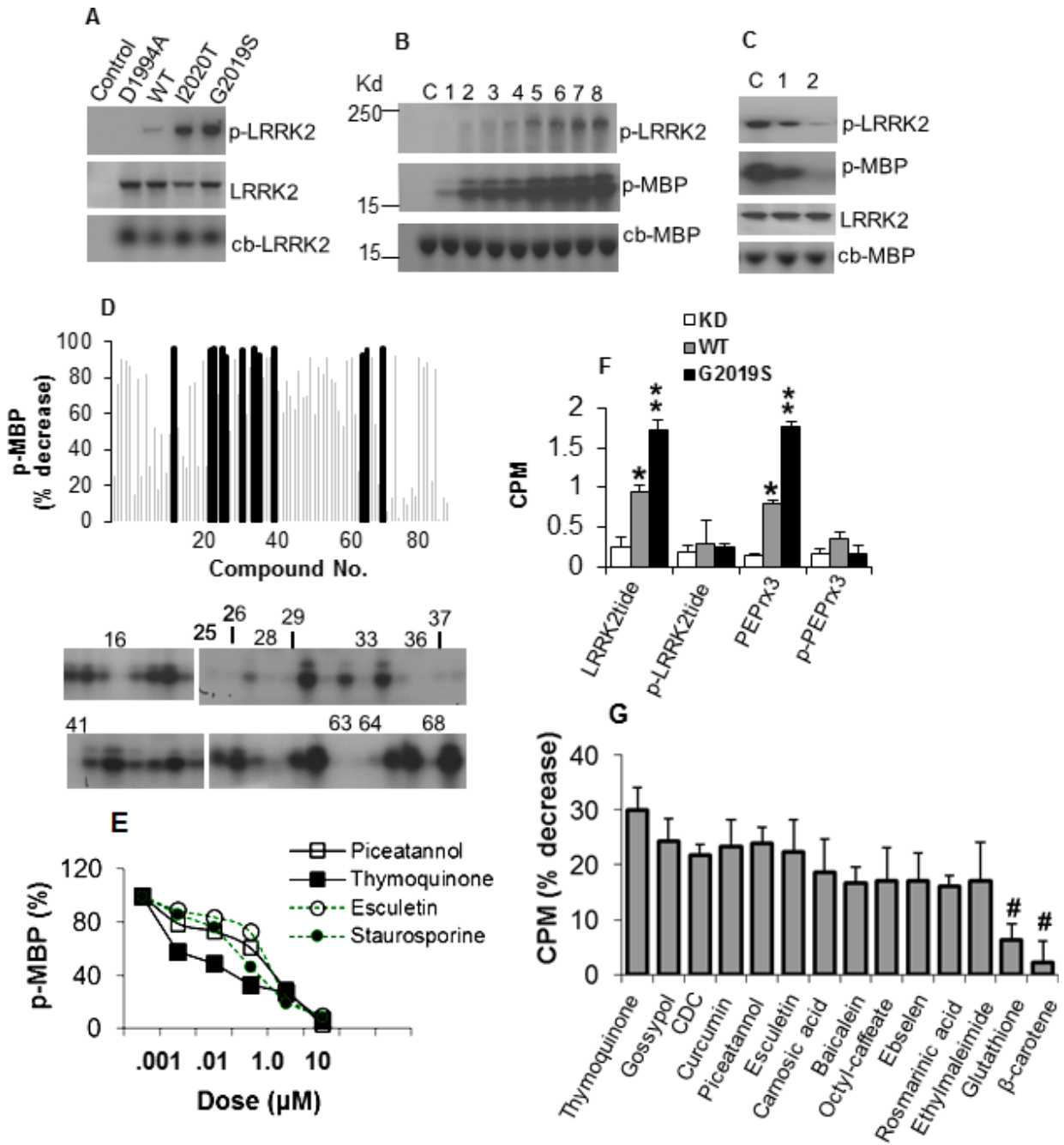


**Figure 1.** Antioxidants inhibit LRRK2 kinase activity. (A) Autoradiogram showing levels of p-LRRK2 in LRRK2 variants (top panel), LRRK2 detected by specific antibody (middle panel) and colloidal blue stain (lower panel). (B) Kinase activity of G2019S on MBP with increasing ATP. Lanes 1–8 contain 0.25, 0.5, 1, 2, 4, 6, 8, 10  $\mu\text{mol/L}$  ATP, respectively. C, no ATP. (C) Inhibition of kinase activity by staurosporine. Lanes 1 and 2 contain  $10^{-3}$  and  $10^{-1}$   $\mu\text{mol/L}$  staurosporine. C, no inhibitor. (D) Antioxidants inhibit G2019S activity on MBP. Chart shows percent decrease in MPU of p-MBP relative to vehicle control (SEM range  $\pm 4.3$ – $12.6$ , not shown for clarity). Blocked bars represent antioxidants exhibiting reduction at  $P < 0.01$ , and correspond to the antioxidant number label on the representative autoradiogram showing the level of p-MBP. (E) Dose–response curves of G2019S-mediated MBP phosphorylation as percent of no inhibitor control in the presence of antioxidants. (F) Activity of LRRK2 variants on phosphorylated and nonphosphorylated peptides in the filter-binding assay, as mean CPM  $\pm$  SEM ( $n = 4$ ) of phosphorylated peptide. \*\*\*Significant increase from KD at  $P < 0.05$  and  $< 0.01$ . (G) G2019S activity on LRRKtide in the presence of antioxidants as percent decrease in CPM  $\pm$  SEM, corrected from and normalized to control without inhibitor. All values were significant at  $P < 0.01$  except for Glutathione and  $\beta$ -carotene (#). LRRK2, leucine-rich repeat kinase-2; p-LRRK2, phosphorylated LRRK2; MBP, myelin basic protein; MPU, mean pixel unit; p-MBP, phosphorylated MBP; CPM, counts per minute.

MBP (p-MBP) substrate (Fig. 1B) showing ATP as a rate-limiting factor. LRRK2 inhibitor *bis*-indole staurosporine reduced kinase activity owing to its nonselective affinity to kinases (Fig. 1C).

### Screening of antioxidants with kinase inhibitor function

To identify inhibitors, we measured p-MBP in the absence or presence of 84 compounds with antioxidant properties. Twelve compounds reduced p-MBP by  $\geq 92\%$ , of which nine are phenolic antioxidants including those in the coumarin and flavonoid subclass and its oxidized derivative quinone, two radical scavengers and a peroxidase mimetic (Fig. 1D, Table S1). Other phenolic inhibitors including Curcumin,  $\gamma$ -Tocopherol, and *n*-Octyl caffeate reduced p-MBP by  $\sim 90\%$ . Weak or noninhibitory compounds include the phenolic probucol, nonphenolic radical scavenger  $\beta$ -carotene, thiol-containing reductant glutathione and those in the nitroxyl radical, metal chelator, and lazaroid groups (Fig. 1D, Table S1). Increasing amounts of compounds mediated proportional decrease in p-MBP with half maximal inhibitory concentration at nanomolar range (Fig. 1E, Table S2), comparable to other reported inhibitors.<sup>10</sup> Thymoquinone exhibited  $IC_{50}$  of 125 and 673 nmol/L against LRRK2-G2019S and -WT, respectively.

### Validation of antioxidant inhibition of kinase activity on LRRK2 substrates

We further tested the antioxidant effect on LRRK2 activity toward its peptide substrates LRRKtide that contains phosphosite T558 in moesin<sup>12</sup> and PEPrx3 with T146 in PRDX3.<sup>11</sup> G2019S showed increased phosphorylation of LRRKtide and PEPrx3, but not the phosphorylated peptides (Fig. 1F). In the presence of antioxidants, kinase activities toward LRRKtide and PEPrx3 were most significantly reduced by piceatannol, rosmarinic acid, thymoquinone, baicalein, gossypol, and esculetin (Fig. 1G, Table S3). Seven antioxidants were able to inhibit kinase activity for LRRKtide, PEPrx3 and MBP. Out of these, we selected thymoquinone (quinone), piceatannol (phenolic), and esculetin (coumarin) from their representative classes for further validation in neuronal and transgenic models.

### Validation of antioxidants in mutant human DA and primary cortical neurons

Next, we tested the effect of lead antioxidants in G2019S-induced death in neurons. The viability of G2019S-expressing human DA neuroblastoma cells and primary cortical neurons decreased by up to 24% showing mutant-induced toxic gain of function (Fig. 2A). However, equimolar sub-

toxic dose of antioxidants improved the viability in G2019S-expressing cells at a *P* value range of 0.0198–0.0106 (Fig. 2B). The number of live cells increased with increasing doses of lead antioxidants (Fig. 2C) suggesting protection from the cytotoxic effect of G2019S.

### Validation of antioxidants in LRRK2 *Drosophila* model

Since LRRK2-G2019S induces mitochondrial oxidative stress,<sup>11,13</sup> we tested the effect of lead antioxidants on the redox state in brain lysates. Piceatannol ( $20,061 \pm 2910$ ), thymoquinone ( $18,445 \pm 1229$ ), and esculetin ( $20,220 \pm 1909$ ) significantly reduced the level of  $H_2O_2$  compared to control ( $31,756 \pm 4142$ ) (Fig. 2D). The level of peroxidase activity was increased by up to 1.7-fold suggesting improvement in overall oxidative state.

To assess the effects of the kinase inhibitory antioxidants, we challenged the LRRK2 G2019S-expressing transgenic flies that previously showed loss in DA neurons compared to LRRK2 WT-expressing and control lines.<sup>13</sup> In each brain hemisphere, we counted the number of DA neurons which form a well-developed network detectable by tyrosine hydroxylase (TH) antibody. At 60-days posteclosion (dpe), the number of TH+ neurons in the protocerebral posterior medial (PPM)1/2, PPM3, and PPL1 (protocerebral posterior lateral 1) clusters of G2019S flies was reduced by 35%, 42%, and 11%, relative to driver control. The addition of lead antioxidants in the diet was protective as the number of neurons in PPM3 in piceatannol, thymoquinone, and esculetin treated G2019S flies increased significantly by up to 55% (Fig. 2E, chart and images) suggesting amelioration of LRRK2 toxicity on DA neurons. The phenolic antioxidant probucol which showed no effect on substrate-directed phosphorylation by G2019S, did not improve the viability of TH+ neurons.

We tested the motor ability which is impaired in G2019S flies with mitochondrial defects.<sup>10</sup> In the presence of antioxidants, the sluggish uncoordinated movement improved with climbing scores increased by up to 22% in piceatannol-treated and 17% in thymoquinone-treated G2019S flies (Fig. 2F), suggesting preservation of mitochondrial redox potential. Furthermore, the G2019S-induced decrease in lifespan was reversed in flies fed with lead antioxidants (Fig. 2G). This was not observed in probucol-fed flies which mediated a nonsignificant 11% decrease in lifespan.

## Discussion

Oxidative stress is one of the pathologic hallmarks of PD.<sup>14</sup> The efficacy of antioxidants in PD has been debated since their results in clinical trials have been equivocal.<sup>15</sup>

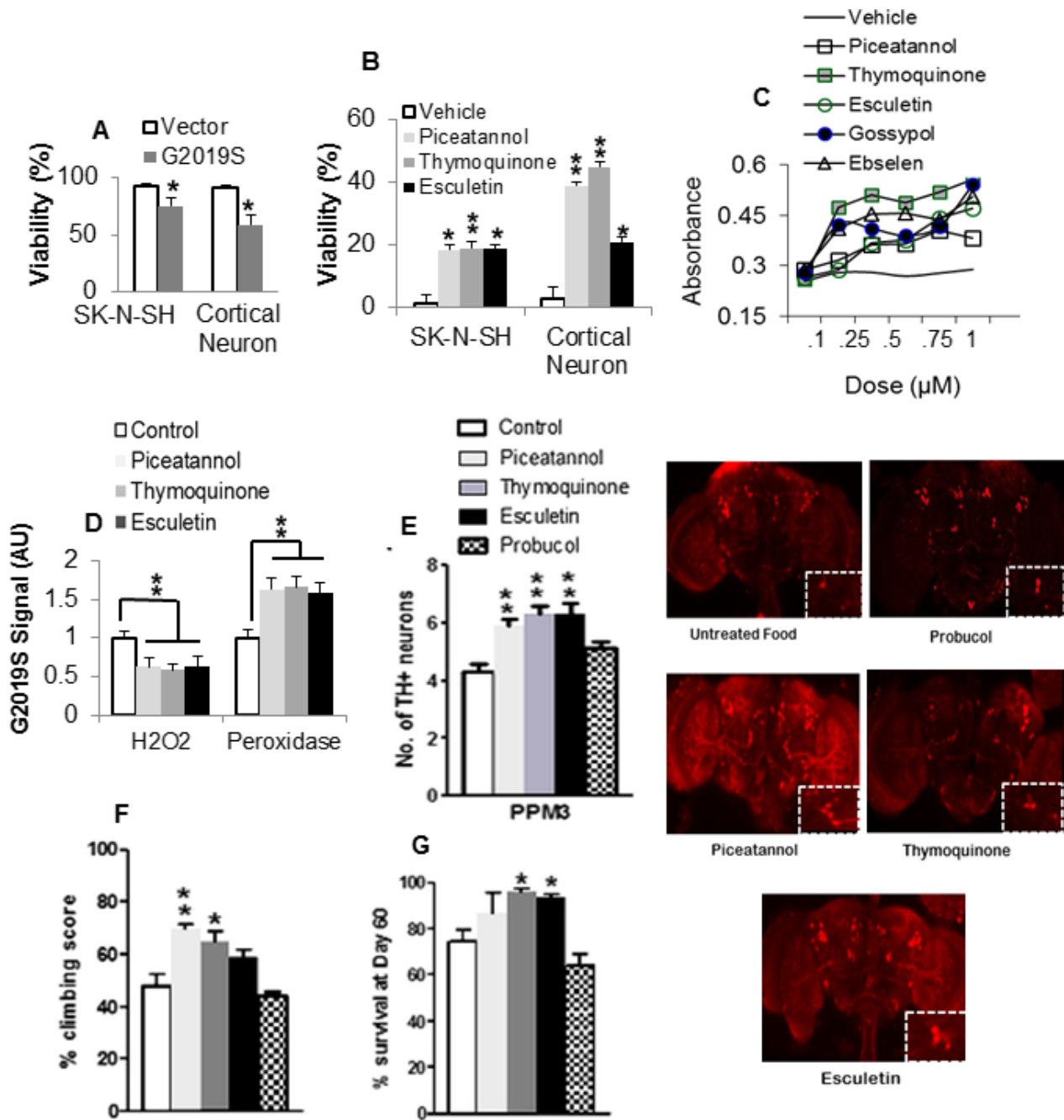


**Figure 2.** Antioxidants ameliorate G2019S-induced neuronal pathologies. (A) Effect of G2019S on viability of human neuronal cells as percent absorbance of untransfected control. \*Significant decrease from control at  $P < 0.05$ . (B) Effect of antioxidants on the viability of G2019S-expressing neurons. Chart shows percent increase in viability as absorbance of antioxidant-treated corrected for and normalized to vehicle-treated control value. \*\*\*Significant increase from control at  $P < 0.05$  and  $< 0.01$ . (C) Dose–response curves of Formazan density in G2019S-expressing SKN-SH cells pretreated with vehicle or increasing amounts of antioxidant. (D) Effect of antioxidants on oxidative state in G2019S brain lysates as relative fluorescence normalized to staple diet-fed control. \*\*Significant at  $P < 0.01$  by one-way ANOVA with Tukey’s multiple comparisons. (E) Number of DA neurons as mean count per cluster ( $n = 4$ ; cohort of 20) in antioxidant or staple diet-fed G2019S control flies. Confocal images of whole-mount brains 60 days after eclosion with magnified views of PPM3 cluster (boxed). Note that the legend applies to succeeding figures (F and G). (F) Climbing scores as percent of mean score normalized to surviving population ( $n = 4$ , cohort of 60). (G) Percentage of surviving flies. ( $n = 4$  cohort of 60). \*\*\*Significant increase from control at  $P < 0.05$  and  $< 0.01$ . ANOVA, analysis of variance; DA, dopamine; PPM, protocerebral posterior medial.



Select natural antioxidants with additional properties such as kinase inhibitor activity,<sup>16</sup> independent of their antioxidant effect may provide an added advantage in preventing neurodegeneration.

Here, we screened 84 antioxidants using p-MBP as a surrogate marker for LRRK2 kinase activities and 12 of these mostly phenolic antioxidants were identified as potent inhibitors. We next validated seven of these antioxidants for their capacity to inhibit kinase activity on previously identified LRRK2 substrates LRRKtide and PEPrx3. Piceatannol, thymoquinone, and esculetin from representative subclasses improved viability in G2019S-expressing DA and primary cortical neurons, rescued dopaminergic neurodegeneration and improved climbing scores and lifespan in transgenic *Drosophila*-expressing human G2019S.

While relevant, inhibitor data must be interpreted with caution as drug discovery efforts in PD are confounded by issues of off-target activities, inconsistent potency due to variability in assay components and parameters used, poor brain bioavailability and toxicity concerns.<sup>10</sup> Indeed, while antioxidants are widely available and safe at dietary level, poor outcomes in clinical trials due to low bioavailability has been suggested,<sup>17</sup> possibly due to experimental use of native compound instead of their active metabolites which could directly interact in relevant pathways.

Polyphenols from diverse groups including flavonoids have displayed antioxidant and physiological mechanistic roles. Piceatannol, thymoquinone, and esculetin are antioxidant compounds that are found naturally in plants and daily consumption is not detrimental to the human body.<sup>17–19</sup> No clinical trials for these compounds have been carried out in PD patients and there are limited experimental data using dopaminergic neurons, although thymoquinone and esculetin readily cross the blood–brain barrier and have been shown to protect dopaminergic neurons against MPP+ in the mouse.<sup>19,20</sup> There has been no previous study of piceatannol in dopaminergic neurons, though it can act as kinase inhibitor.<sup>16</sup> Theoretically, natural antioxidants that are present in many foods confer less toxicity and brain permeability concerns.

In conclusion, using a systemic approach, we have provided proof of principle that natural antioxidants with dual antioxidant and kinase inhibitor properties could be potentially useful for LRRK2-linked PD. While their inhibitor properties may not be specific, their toxicity is of less concern than clinically untested kinase inhibitors. However, their potential off-target effects should be further evaluated. In this alternative class of potentially therapeutic drugs, careful derivation of active metabolites that could enhance delivery and bioavailability may pave the way for clinical trials in LRRK2 mutant carriers.

## Acknowledgments

We thank all staffs who have helped with the project and the National Medical Research Council (National Research Foundation Star award and translational clinical research program in Parkinson's disease) for their support.

## Authors' Contributions

Drs E.-K. Tan and Angeles planned the study, Angeles, Ho, Lim and Dymock helped with the methodology and experiments. E.-K. Tan and Angeles drafted the manuscript and all authors contributed to the final version.

## Conflict of Interest

There are no potential conflicts of interest to declare. E.-K. Tan has received honoraria for editorial work in the European journal of Neurology and Parkinsonism related disorders.

## References

1. Lees AJ, Hardy J, Revesz T. Parkinson's disease. *Lancet* 2009;373:2055–2066.
2. Dickson DW, Braak H, Duda JE, et al. Neuropathological assessment of Parkinson's disease: refining the diagnostic criteria. *Lancet Neurol* 2009;8:1150–1157.
3. Tarazi FI, Sahli ZT, Wolny M, Mousa SA. Emerging therapies for Parkinson's disease: from bench to bedside. *Pharmacol Ther* 2014;144:123–133.
4. Tan EK, Skipper LM. Pathogenic mutations in Parkinson disease. *Hum Mutat* 2007;28:641–653.
5. Chan SL, Angeles DC, Tan EK. Targeting leucine-rich repeat kinase 2 in Parkinson's disease. *Expert Opin Ther Targets* 2013;17:1471–1482.
6. Piccoli G, Condliffe SB, Bauer M, et al. LRRK2 controls synaptic vesicle storage and mobilization within the recycling pool. *J Neurosci* 2011;31:2225–2237.
7. MacLeod D, Dowman J, Hammond R, et al. The familial Parkinsonism gene LRRK2 regulates neurite process morphology. *Neuron* 2006;52:587–593.
8. Stafa K, Trancikova A, Webber PJ, et al. GTPase activity and neuronal toxicity of Parkinson's disease-associated LRRK2 is regulated by ArfGAP1. *PLoS Genet* 2012;8:e1002526.
9. Chan SL, Chua LL, Angeles DC, Tan EK. MAP1B rescues LRRK2 mutant-mediated cytotoxicity. *Mol Brain* 2014;7:29.
10. Kramer T, Lo Monte F, Göring S, et al. Small molecule kinase inhibitors for LRRK2 and their application to Parkinson's disease models. *ACS Chem Neurosci* 2012;3:151–160.

11. Angeles DC, Gan B-H, Onstead L, et al. Mutations in LRRK2 increase phosphorylation of peroxiredoxin 3 exacerbating oxidative stress-induced neuronal death. *Hum Mutat* 2011;32:1390–1397.
12. Jaleel M, Nichols RJ, Deak M, et al. LRRK2 phosphorylates moesin at threonine-558: characterization of how Parkinson's disease mutants affect kinase activity. *Biochem J* 2007;405:307–317.
13. Angeles DC, Ho P, Chua LL, et al. Thiol peroxidases ameliorate LRRK2 mutant-induced mitochondrial and dopaminergic neuronal degeneration in *Drosophila*. *Hum Mol Genet* 2014;23:3157–3165.
14. Dias V, Junn E, Mouradian MM. The role of oxidative stress in Parkinson's disease. *J Parkinsons Dis* 2013;3:461–491.
15. Schapira AH, Patel S. Targeting mitochondria for neuroprotection in Parkinson disease. *JAMA Neurol* 2014;71:537–538.
16. Geahlen RL, McLaughlin JL. Piceatannol (3,4,3',5'-tetrahydroxy-trans-stilbene) is a naturally occurring protein-tyrosine kinase inhibitor. *Biochem Biophys Res Commun* 1989;165:241–245.
17. Kidd PM. Bioavailability and activity of phytosome complexes from botanical polyphenols; the silymarin, curcumin, green tea, and grape seed extracts. *Altern Med Rev* 2009;14:226–246.
18. Bhullar KS, Rupasinghe HP. Polyphenols: multipotent therapeutic agents in neurodegenerative diseases. *Oxid Med Cell Longev* 2013;2013:891748.
19. Radad K, Moldzio R, Taha M, Rausch WD. Thymoquinone protects dopaminergic neurons against MPP+ and rotenone. *Phytother Res* 2009;23:696–700.
20. Subramaniam SR, Ellis EM. Neuroprotective effects of umbelliferone and esculetin in a mouse model of Parkinson's disease. *J Neurosci Res* 2013;91:453–461.

## Supporting Information

Additional Supporting Information may be found in the online version of this article:

**Table S1.** Antioxidant inhibitors of G2019S kinase activity on MBP.

**Table S2.** Structure and IC<sub>50</sub> of lead antioxidants on MBP.

**Table S3.** Antioxidant inhibitors of G2019S kinase activity on substrate-derived peptides.